frontiers | Frontiers in Ecology and Evolution

TYPE Original Research
PUBLISHED 08 December 2023
DOI 10.3389/fevo.2023.1227020

OPEN ACCESS

EDITED BY
Laura Parducci,
Sapienza University of Rome, Italy

REVIEWED BY
Keely Mills,
The Lyell Centre, United Kingdom
Neal Michelutti,
Queen's University, Canada
Thomas A. Minckley,
University of Wyoming, United States

*CORRESPONDENCE
Antonio Maldonado
antonio.maldonado@ceaza.cl

RECEIVED 22 May 2023
ACCEPTED 17 November 2023
PUBLISHED 08 December 2023

CITATION
Martel-Cea A, Maldonado A, de Porras ME, Muñoz P, Maidana NI, Massaferro J and Schittek K (2023) A multiproxy approach to reconstruct the Late Holocene environmental dynamics of the semiarid Andes of central Chile (29°S). *Front. Ecol. Evol.* 11:1227020. doi: 10.3389/fevo.2023.1227020

A multiproxy approach to reconstruct the Late Holocene environmental dynamics of the semiarid Andes of central Chile (29°S)

Alejandra Martel-Cea[1,2], Antonio Maldonado[1,3]*, María Eugenia de Porras[4], Praxedes Muñoz[3], Nora I. Maidana[5,6], Julieta Massaferro[7] and Karsten Schittek[8]

[1]Laboratorio de Paleoecología y Paleoclimatología, Centro de Estudios Avanzados en Zonas Áridas (CEAZA), La Serena, Chile, [2]Laboratorio de Palinología y Reconstrucciones Ambientales, Instituto Ciencias de la Tierra, Universidad Austral de Chile, Valdivia, Chile, [3]Departamento de Biología Marina, Universidad Católica del Norte, Coquimbo, Chile, [4]Instituto Argentino de Nivología, Glaciología y Ciencias Ambientales – Consejo Nacional de Investigaciones Científicas y Técnicas de Argentina (IANIGLA-CONICET), Mendoza, Argentina, [5]Laboratorio de Diatomeas Continentales, Facultad de Ciencias Exactas y Naturales, Departamento de Biodiversidad y Biología Experimental, Universidad de Buenos Aires, Buenos Aires, Argentina, [6]Laboratorio de Diatomeas Continentales, Consejo Nacional de Investigaciones Científicas y Técnicas de Argentina (CONICET) – Universidad de Buenos Aires, Instituto de Biodiversidad y Biología Experimental y Aplicada (IBBEA), Buenos Aires, Argentina, [7]Programa de Estudios Aplicados a la Biodiversidad del Parque Nacional Nahuel Huapi – Consejo Nacional de Investigaciones Científicas y Técnicas de Argentina (CENAC-CONICET), Bariloche, Argentina, [8]Institute of Geography Education, University of Cologne, Cologne, Germany

Mountain ecosystems located in the Andes cordillera of central Chile (29–35°S) have been strongly affected by the ongoing Mega Drought since 2010, impacting the snow cover, the surficial water resources (and thereby water storage), as well as the mountain biota and ecosystem services. Paleoenvironmental records in this part of the semiarid Andes are key to estimating the effects of past climate changes on local communities helping to forecast the ecological and biological responses under the aridification trend projected during the 21st century. Here we present a 2400-year multiproxy paleoenvironmental reconstruction based on pollen, diatoms, chironomids, sedimentological and geochemical data (XRF and ICP-MS data) of Laguna El Calvario (29°S; 3994 m a.s.l), a small and shallow Andean lake. Four main hydrological phases were established based on changes in the lithogenic and geochemical results associated with allochthonous runoff input and the subsequent response of the biological proxies. Between 2400 and 1400 cal yrs BP, wetter than present conditions occurred based on the intense weathering of the lake basin and the dominance of upper Andean vegetation. A decrease in moisture along with sub-centennial discrete wet pulses and lake-level changes occurred until ~800 cal yrs BP followed long-term stable climate conditions between 1850 and 1950 AD as suggested by a drop in vegetation productivity and low lake levels. From 1950 AD to the present, a decline in moisture with a severe trend to drier conditions occurring in the last decades occurred as reflected by an upward vegetation belt displacement around Laguna El Calvario along with a turnover of diatom assemblages and high productivity in the water column.

KEYWORDS

semiarid Andes, climate change, multiproxy analysis, mountain ecosystems, lake sediments, Late Holocene

1 Introduction

Low water availability and uncontrolled changes in land use and cover are becoming the main stressors in semiarid western Andes (29°–34°S) ecosystems under the ongoing scenario of climatic change. In this regard, the desertification process is critical in the northernmost area (especially in the Coquimbo region; 29°–32°S) (Emanuelli et al., 2016; Pizarro-Tapia et al., 2021) given that it has negatively affected the biodiversity and the ecosystem services (e.g., socioeconomic activities). The Andes cordillera acts as a water reservoir of solid/liquid precipitation falling during a few rainy months and therefore, its role has taken key relevance under the decline of precipitation and rise of temperatures in the past decades (Falvey and Garreaud, 2009; Quintana and Aceituno, 2012; Barria et al., 2019; Garreaud et al., 2019). Given that those trends will be accentuated during the 21st century causing a reduction in the snow cover as well as in glacier extension and mass balance, the projected decrease in streamflow (water supply) to the lowlands is critical (Vicuña et al., 2011).

To have a deep comprehension of how climate-sensitive high mountain ecosystems in the semiarid Andes will respond to future climate change in the mid-to-long term scale, it is necessary to understand past environmental dynamics. Despite the scarce high-elevation paleoenvironmental records in the semiarid Andes, those published in the last decade have helped to infer hydrological changes associated with the latitudinal dynamics of the northern border of the Southern Westerly Winds (SWW) and its interaction with the Southeast Pacific Subtropical Anticyclone (SEPSA) (Martel-Cea et al., 2016; Tiner et al., 2018; Mayta and Maldonado, 2022). Pollen records from central Chile (33°–36°S) suggested a high short-term variability during the Late Holocene attributed to an increased frequency of El Niño Southern Oscillation (ENSO) events (Jenny et al., 2002a; Maldonado and Villagrán, 2006; Frugone-Álvarez et al., 2020; Muñoz et al., 2020). The establishment of the modern semiarid conditions occurred around 600–700 calibrated years before the present (hereafter cal yrs BP) in the semiarid Andes (Martel-Cea et al., 2016; Mayta and Maldonado, 2022).

This work therefore presents a new Late Holocene environmental reconstruction from a high-altitude lacustrine record in the semiarid Andes (29°S) based on a multiproxy approach. Sedimentological and geochemical proxies such as organic/inorganic matter content and trace elements along with biological proxies such as pollen, diatoms, and chironomids were analyzed. Specifically, Laguna El Calvario was chosen because of its high sensitivity to changes in the snow cover (the main source of water input to the lake) which further allows for the reconstruction of long-term changes in the past 2400 years in hydrology and limnological conditions.

2 Study area

Laguna El Calvario (29°34'7.63" S; 70°21'8.63" W, 3994 m a.s.l., depth ca. 1 m, 0.8 ha area) is a small closed shallow lake located at the head of a west–east oriented valley called Quebrada Matancilla in the semiarid Andes of central Chile (Figure 1). The lake is flanked by Pleistocene-Holocene glacier deposits. The surrounding hills and basal bedrock consist of K-rich intrusive plutonic rocks of the Permian period [Guanta plutonic complex Peg(t) and Peg(gd)] which are mainly composed of tonalite and granodiorite (Nasi et al., 1985; Murillo et al., 2017). Indeed, industrial mining activities for the exploitation of Cu, Au, and Fe have been developed during the last 100 years in the semiarid Andes of central Chile (SERPLAC, 1986) having important effects on high Andean ecosystems (e.g., on natural water reservoirs; Oyarzún et al., 2006).

The climate of the study area is cold semiarid with Mediterranean influence characterized by cold/wet winters and dry/warm summers. Annual precipitation reaches 130 mm (JJA:

FIGURE 1
(A) South America and central Chile map showing the location of Laguna El Calvario (LCA) and some of the sites mentioned in the text; **(B)** 3D image of the Laguna El Calvario valley (DEM ALOS PALSAR SRTM 12.5 m JAXTA); and **(C)** photograph of Laguna El Calvario from the west.

60%) while the mean annual temperature is 3.8°C (DJF: 7.7°C; JJA: 0°C) (CRU 1980–2016). Winter precipitation originates from frontal systems associated with the northern border of the Southern Westerlies belt and is modulated by its interaction with the subtropical Anticyclone. While the frontal systems migrate in the NW-SE direction, they are intercepted by the Andes cordillera causing a strong rainfall gradient along the west side of the Andes (orographic enhancement) (Falvey and Garreaud, 2007). As the mean annual altitude of the 0°C isotherm at 29°S is located at ~4300 m a.s.l. (Carrasco et al., 2005; Barria et al., 2019), most of the precipitation around Laguna El Calvario falls as snow. During summertime, rainfall events are less frequent and correspond to convective storms coming from the eastern side of the Andes Cordillera accounting for less than 10% of the annual precipitation (Garreaud and Rutllant, 1997; Viale and Garreaud, 2014). However, summer storms bring fresh snow and cloud cover that reduce the albedo (and therefore sublimation), diminishing glacier melting in the semiarid Andes (Abermann et al., 2014). The climate interannual-to-quasidecadal variability in the area is strongly influenced by the El Niño Southern Oscillation (ENSO; positive phase), which is responsible for higher-than-average amounts of winter precipitation (Aceituno, 1988; Montecinos and Aceituno, 2003; Garreaud, 2009; Quintana and Aceituno, 2012). The high correlation between the warm ENSO phase and above-average accumulation of snowpack, increased streamflow, and positive glacier mass balance have relieved the arid trend observed in the last decades in the subtropical semiarid Andes (Masiokas et al., 2006; Gascoin et al., 2011). On the other hand, the Southern Annular Mode (SAM) in its negative (positive) phase promotes higher(lower)-than-average precipitation in south-central Chile (Quintana and Aceituno, 2012).

The vegetation composition and distribution follow the steep gradient of the semiarid Andes (so-called vegetation belts) linked to the abrupt changes in temperature, precipitation, topography (such as slope orientation), and soil characteristics. Both species diversity and plant cover decline with elevation due to the extreme conditions in the high Andean environments (Villagrán et al., 1983; Arroyo et al., 1988; Squeo et al., 1993; López-Angulo et al., 2018). On the other hand, the length of the growing season also shortens with elevation and the maximum primary productivity is recorded from the late spring (Nov–Dec) to late summer (March) (Squeo et al., 1994; Rudloff et al., 2021). Following the biogeographic data provided by Luebert and Pliscoff (2017) and the terminology of Squeo et al. (1994), it is possible to differentiate three main vegetation belts:

Pre-Andean belt (<2700m a.s.l.), characterized by major life forms such as shrubs, cacti, perennial and annual herbs. The most common species are *Ephedra chilensis, Colliguaja odorifera*, *Adesmia confusa*, *A. microphylla, Haplopappus angustifolius, Cumulopuntia sphaerica.* Tree species are restricted to azonal areas (meadows in ravines). This vegetation belt is strongly disturbed by anthropic activities and the vegetation cover reaches up to 40%.

Sub-Andean belt (2700–3500 m a.s.l.), the major life forms are shrubs and perennial herbs such as *Senecio proteus, Haplopappus baylahuen, Ephedra breana, Chuquiraga ulicina, Adesmia parviflora, A. hystrix. Atriplex imbricata, Chaetanthera limbate, Fabiana viscosa, F. imbricata, Viviania marifolia*, and *Cristaria andicola*. Tree species may appear in meadows up to 2900 m. This belt also has a cover ca. 40%.

Andean belt (3500–4450 masl) dominated by shrubs, perennial herbs, and cushion plants can be further divided into the lower and upper Andean belt. The lower Andean belt (up to 4250 m; cover ca. 27%) is characterized by *Adesmia subterranea, A. echinus, A. aegiceras*, *Azorella madreporica, Stipa chrysophylla, S. frigida*, *Cistanthe picta, Chaetanthera minuta*, and *C. sphaeroidalis.* The upper Andean belt (4250–4450 m: cover ca. 0.7%) is mainly composed of perennial herbs and grasses and a few dwarf shrubs such as *Chaetanthera sphaeroidalis*, *C. pulvinate, Stipa frigida, Adesmia subterranea, A. capitellata, Senecio pissisii*, and *S. socompae.*

3 Methodology

3.1 Coring and sedimentological, chronological, and geochemical analyses

Four short cores of Laguna El Calvario (LCA) were retrieved in 2017 using a UWITEC© gravity corer. All the cores were lithologically characterized through X-radiographs and visual descriptions. The LCA SHC-4 core was selected for performing the multiproxy analysis given it was the longest (33 cm long; Figure 1 Supplementary Material). The sedimentological analysis included a loss on ignition, X-ray fluorescence analysis (XRF), and inductively coupled plasma mass spectrometry (ICP-MS). Loss-on ignition was assessed at a contiguous 1 cm interval to estimate organic, inorganic, and carbonate contents (Heiri et al., 2001). The chronology of the Laguna El Calvario record was established through ^{210}Pb and ^{14}C dating techniques. The ^{210}Pb activities (dpm g^{-1}) were estimated for the first 15 cm through its daughter radionuclide ^{210}Po which is in secular equilibrium (Table 1 Supplementary Material). The chemical procedure included the acid digestion of sediment samples with the addition of ^{209}Po as a yield tracer and the deposition of the ^{210}Po onto ultrapure silver discs (Flynn, 1968). Activities were quantified in a Canberra Quad Alpha Spectrometer until a 1 σ error was achieved. Additionally, five bulk sediment samples were analyzed for AMS radiocarbon dating in the Direct AMS laboratory, USA. Levels 0–1 cm and 6–7 cm were analyzed for the ^{14}C measurements in order to check any ^{14}C reservoir effect, a common issue in high Andean lakes. According to the ^{210}Pb model these levels correspond to the second half of the 20th century, −60 and −9 cal yrs BP, respectively. To estimate the reservoir effect in the Laguna El Calvario, the ^{14}C ages from levels 0–1 cm and 6–7 cm were averaged resulting in a reservoir age of 1041 ^{14}C yrs BP (950 cal yrs BP), which was subtracted from the remaining three older radiocarbon ages (Table 1). Then, the radiocarbon ages were calibrated with the SHCal20 curve (Hogg et al., 2020) and the age-depth model was computed using Plum (Aquino-López et al., 2018) with the rPlum R package (Blaauw et al., 2020). rPlum is a recently developed Bayesian approach that permits computing integrated

TABLE 1 AMS radiocarbon dates of Laguna El Calvario record for the core LCA SHC4 core.

Laboratory ID	Sample ID	Depth (cm)	Material	^{14}C age	Corrected cal. ages	^{210}Pb ages (mid-point)
D-AMS 021485	LCA SHC4 0–1cm	0–1	Bulk sediment	544 ± 28	–	−60
D-AMS 021486	LCA SHC4 6–7cm	6–7	Bulk sediment	1598 ± 21	–	−9
D-AMS 021487	LCA SHC4 18–19cm	18–19	Bulk sediment	2008 ± 31	937	
D-AMS 021488	LCA SHC4 28–29cm	28–29	Bulk sediment	2549 ± 51	1478	
D-AMS 021489	LCA SHC4 32–32.5cm	32–32.5	Bulk sediment	3765 ± 49	2694	

chronologies without pre-modeling the ^{210}Pb ages but combining other chronostratigraphic markers such as the ^{14}C ages.

The XRF scanning was employed to measure the variability of geochemical elements on unprocessed sediments using an ITRAX core scanner (Cox Analytical Systems, Croudace et al., 2006) at the GEOPOLAR laboratory of the University of Bremen, Germany. Measures of the XRF series were established at each 2 mm interval and then a molybdenum tube at 40 kV and 10 mA was applied with an exposure time of 5 s for every measurement. The concentration of the different minerals was expressed in total counts (cnts) and elements over 100 cnts were selected. To support XRF data, continuous and discrete sediment samples were analyzed using an ICP-MS at UC-Davis facilities, from total digested sediment samples. The chemical procedure briefly consists of digesting ~250 mg of sediment with a mix of strong high-purity acids (HNO_3, HCl, $HCLO_4$, HF; Suprapure®Merck) in several steps until total dissolution, using screw-top PFA-Teflon™ vials and a hotplate Teflon™ PFA coating.

3.2 Inorganic proxies

Water content, organic matter, and grain size influence the scanning densities on XRF analysis (Zhang et al., 2020; Mondal et al., 2021), therefore ICP-MS was used to verify the trends of the measured elements included in this work. The elements Ti, K, Sr, and Rb can be associated with allochthonous detrital input into the lake (Guyard et al., 2007; Davies et al., 2015). The Ti/coh ratio was used as a proxy of clastic input (Ohlendorf et al., 2014; Schittek et al., 2016). The Zr/Ti ratio was used to infer the grain size given that Zr is highly abundant in the coarse silt fraction whereas Ti can be found in the clay to fine-silt fraction (Oldfield et al., 2003). Therefore, high Zr/Ti ratio values indicate increased coarse silt influx (Shala et al., 2014). The Si, P, Cd, U, and Cu elements were standardized by Titanium deposition.

3.3 Biological proxies

Pollen, diatom, and chironomid records were analyzed at 2 cm discrete intervals so each biological proxy record consisted of 17 samples. For the pollen analysis, 1 cm^3 of these sediment samples were processed following the standardized methods outlined by Faegri and Iversen (1989), including KOH treatment, sieving, acids (HCl and HF for carbonate and silicate removal), and acetolysis. In levels with low pollen concentration, an additional 2 cm^3 of sediment was processed. For the estimation of pollen concentration (grains cm^{-3}), tablets of *Lycopodium clavatum* were added to each sediment sample (Stockmarr, 1971). The palynomorphs were determined at the most detailed taxonomic level under a microscope (400–1000×) aided by pollen taxonomic keys (Heusser, 1971; Markgraf and D'Antoni, 1978) and reference samples from the Laboratorio de Paleoecología y Paleoclimatología of the Centro de Estudios Avanzados en Zonas Áridas (CEAZA). The basic pollen sum includes a minimum of 300 terrestrial pollen grains per sample while paludal, aquatic, and/or non-pollen taxa such as zygospores (Zygnemataceae) and microalgae were incorporated in a separate sum. Relative abundances were calculated for each taxon. Pollen accumulation rates (grains cm^{-2} yr^{-1}) were calculated employing the pollen concentration values and sedimentation rate derived from the age-depth model.

Two (2) grams of sediment were processed for diatom analysis following the methodology outlined by Battarbee (1986). Each sample was dried, oxidized with H_2O_2, and heated for 2 minutes in a microwave. Finally, permanent preparations were mounted using Naphrax®. A minimum of 600 valves were counted to determine the relative abundances. For absolute abundances, the aliquot method (Battarbee, 1986) was used, following random transects. Results are expressed in valves per gram of dry sediment. The taxonomic literature on diatom determination included the monographic works of Metzeltin and Lange-Bertalot (1998); Metzeltin and Lange-Bertalot (2007), Rumrich et al. (2000), and Lange-Bertalot et al. (2017), among others.

Five (5) grams of wet sediment were processed for chironomid analysis. The sediment samples were deflocculated using 10% KOH solution at 50–70°C for 30 minutes and sieved through 100 and 200 um mesh sizes. Larval head capsules (HC) were hand-sorted from the residual sediment and mounted on permanent slides with Hidromatrix® mounting media. Taxonomic identification was performed under a Nikon Phase optic microscope at a magnification of 100–1000× with reference to available taxonomic literature (Massaferro and Brooks, 2002; Massaferro et al., 2013; Cranston, 2019).

Given the nature of each of the analyzed proxies in the Laguna El Calvario record, their sensitivity and response time to a given environmental/climatic change may differ from one to another. So we decided to analyze each of them separately and therefore integrate their signal in the discussion section taking into account the different spatial/temporal scales represented by each other.

4 Results

4.1 Chronology, lithology, organic and inorganic content, XRF and ICP-MS analyses

The retrieved core of Laguna El Calvario spans the last 2400 cal yrs BP (Figure 2). The part of the age–depth model based on the three radiocarbon dates is the most accurate possible concerning the given ages (Table 1). The ^{210}Pb radioactive activities showed good exponential decay and the unsupported activities occurred in the first 15 cm reaching the age of 1833 AD (Figure 2, Table 1 Supplementary Material), determining a supported activity of 0.85 ± 0.17 dpm g^{-1}. The mean sedimentation rate ranges around 0.13 ± 0.01 cm year^{-1} in the first 5 cm.

The lithological description and organic content of the sedimentological record of Laguna El Calvario (LCA-SHC4; 33 cm) are summarized in Figure 3. Between 33 and 28 cm the sediment is composed of a porous dark brownish silty sand with gravel-sized clasts. The organic matter and carbonate contents are around 25% and 3%, respectively, while the inorganic density exhibits its highest values (0.21–0.33 g cm^{-3}). The sediment composition shifts to clayey silt from 28 cm to the top of the core. Intercalated light–dark brown and green laminated layers are present around 20–28 cm and 2–8 cm whereas a brown homogeneous layer is present between 20 and 8 cm. The content of organic matter and clasts fluctuates around 22–42%, and 2.6–3.9%, respectively. Inorganic density ranged between 0.1 and 0.2 g cm^{-3}.

Regarding the geochemical results, changes in XRF-Molybdenum Incoherent/Coherent ratio (inc/coh) follow the LOI organic matter (%) and water content (%) (Figure 3). The elements Ti, K and Sr show similar trends throughout the core according both, XRF and ICP-MS data (Figure 4; Tables 2, 3 Supplementary Material), which validates the data obtained with XRF. Indeed, the strong coherence among these curves suggests the same origin of variability (Table 2 Supplementary Material). The sparse plant cover in the surroundings and the hydrological changes associated with the precipitation regime dynamics can modulate the terrigenous input into the lake therefore, the Ti/coh ratio was applied as an indirect indicator of precipitation. Thus, high values of Ti/coh ratio along with Ti, K, and Sr in the ICP-MS were recorded between 32 and 28 cm (Figure 4). Between 28 and 20 cm, Ti/coh ratio shows highly variable values with maxima around 27 and 21 cm concomitant with the occurrence of a dark layer (Figure 4). Between 20 and 8 cm, these ratio values are more stable but show a rising trend. Ti, K, and Sr and the Ti/coh ratio values display a

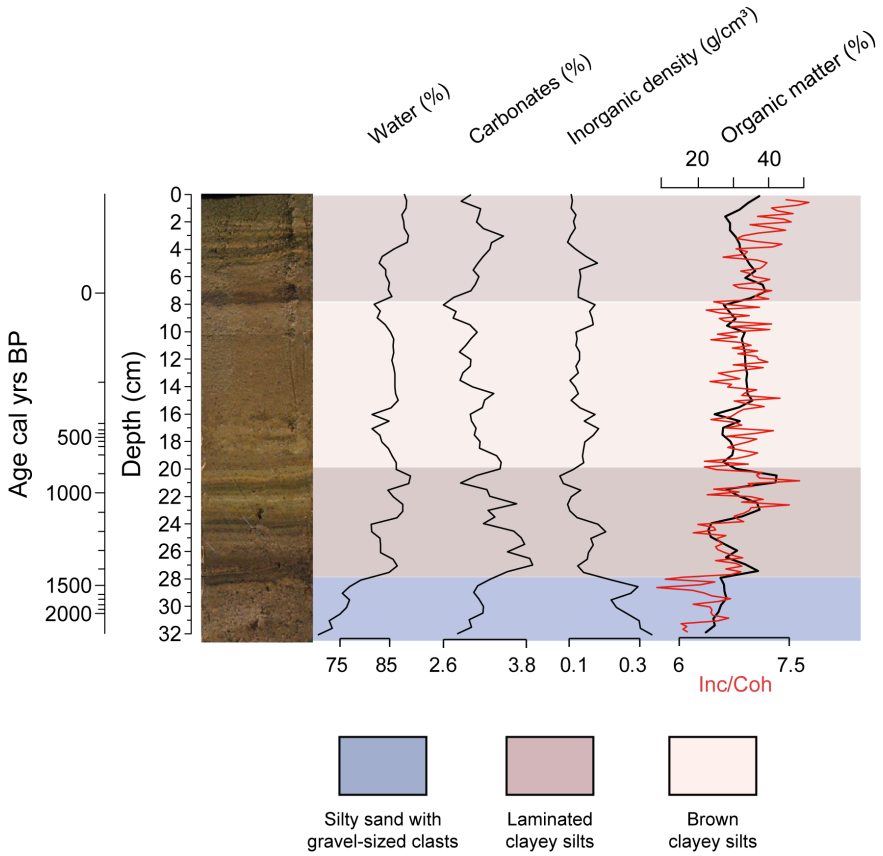

FIGURE 2
Bayesian age *vs* depth model constructed in rplum R package (Blaauw et al., 2020) based on the ^{210}Pb and radiocarbon ages of the LCA SH4 core. The weighted mean of the model is represented in the red dashed line where the black shadow shows the 95% confidence interval. Blue rectangles indicate the depth position and ^{210}Pb activities (dpm g^{-1}) (axis labels at the right) and ^{14}C samples correspond to the purple figures.

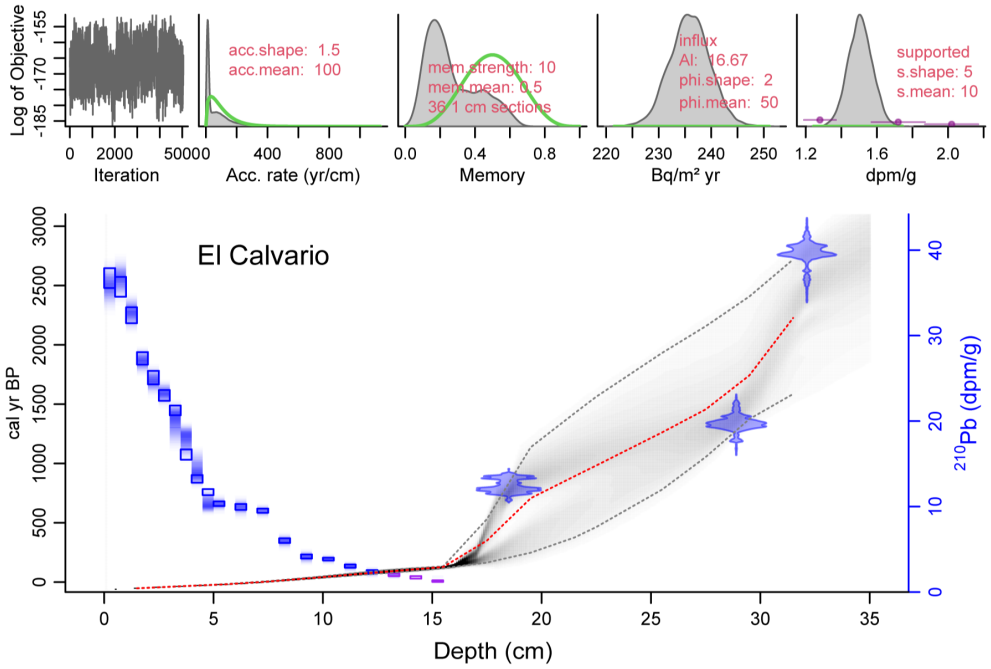

FIGURE 3
Lithology, water content and loss on ignition of the Laguna El Calvario record.

declining trend in the last 8 cm. Additionally, XRF data including Rb showed similar trends (Figure 4).

The Zr/Ti ratio, a proxy of grain size changes, shows peak values and high variability that are concomitant with laminated sediments between 28 and 20 cm and then, in the last 8 cm (Figure 4). The silica data based on the XRF analysis were not included in the results due to the low counts. In this regard, the Si/Ti ratio in the ICP_MS analysis shows different trends of the detrital-related elements since increases are observed in the topmost 6 cm of the record (Figure 4). So, the variation of silica in the record could be attributed to intra-lake processes such as productivity. The P/Ti ratio from the ICP-MS data also shows the highest values in the topmost 6 cm supporting the silica interpretation. The ICP-MS Cd/Ti and U/Ti ratios were considered as proxies of sulfidic conditions and organic sedimentation given that the U content is normally well correlated with organic fluxes reaching the bottom of the lake. In fact, Cd/Ti and U/Ti ratios present their highest values in the topmost 8 cm. Finally, the ICP-MS Cu/Ti is considered an indicator of mining activity in the region, which displays the highest concentrations in the uppermost 6 cm.

4.2 Biological proxy analyses

The palynological record shows a high plant diversity with pollen taxa defining the three main vegetation belts in the western semiarid Andean region: Poaceae, *Adesmia*-type, and *Nassauvia*-type (high and lower Andean); *Ephedra* (sub-Andean), and Chenopodiaceae and arboreal taxa (pre-Andean) (Figure 5A).

Between 32 and 22 cm (2400–1000 cal yrs BP; Figure 5A), the pollen record is dominated by Poaceae (up to 22%), *Chaethantera/Oriastrum* (6–17.3%), *Senecio*-type (6–12%), *Oxalis* (3–11%), *Ephedra* (<10%), Chenopodiaceae (9–14%) and *Arenaria* (4–13%). The cold-tolerant pollen types such as *Nassauvia*-type (up to 3.6%), *Adesmia*-type (up to 6.2%), *Laretia*-type (up to 5%) reach their highest values at the top of the zone (1500–1000 cal yrs BP) whereas Poaceae percentages gradually decline (8.5%). *Arenaria values* increase from 4 to 12% since 1300 cal yrs BP. Cyperaceae and *Myriophyllum*, paludal and aquatic taxa, display low frequencies (<2%) while the non-pollen palynomorph *Pediastrum* presents maximum values of ~28 cm. Pollen accumulation rates (PAR) for local terrestrial taxa are relatively low ranging between 9 and 25 pollen grains cm^{-2} yr^{-1}.

Between 22 and 12 cm (1000–75 cal yrs B; Figure 5A), the pollen assemblages are characterized by the slight recovery of Poaceae values up to 14.5% along with the decline of *Chaethantera/Oriastrum*, *Nassauvia*-type and *Adesmia*-type. *Ephedra* (up to 21.6%), Montiaceae (4–17%) and Verbenaceae (2–7%) values increase during this period. Cyperaceae percentages remain under 2% while *Pediastrum* values strongly decline to almost zero. *Spirogyra* spores display a mild increment and the *Zygnema* spores percentages increase at 16 cm (100 cal yrs BP). PAR values are the lowest for the whole record (total terrestrial pollen ca. 2 grains cm^{-2} yr^{-1}) increasing towards the end of this period (up to 40 grains cm^{-2} yr^{-1}).

Between 12 and 0 cm (75 cal yrs BP to present; Figure 5A), shrubs such as *Ephedra*, Chenopodiaceae, and *Senecio*-type percentages declined at the expenses of Poaceae (10–37%) and herbs values such as *Arenaria* (12–28%) and Montiaceae (13–21.6%). Other taxa percentages such as Verbenaceae (5–10%) and *Plantago* (1–2.5%) increase during this period similar to Cyperaceae percentages that show an increment towards the top of the record (2.6–12.8%). The non-pollen palynomorphs (NPPs), such as the

10.3389/fevo.2023.1227020

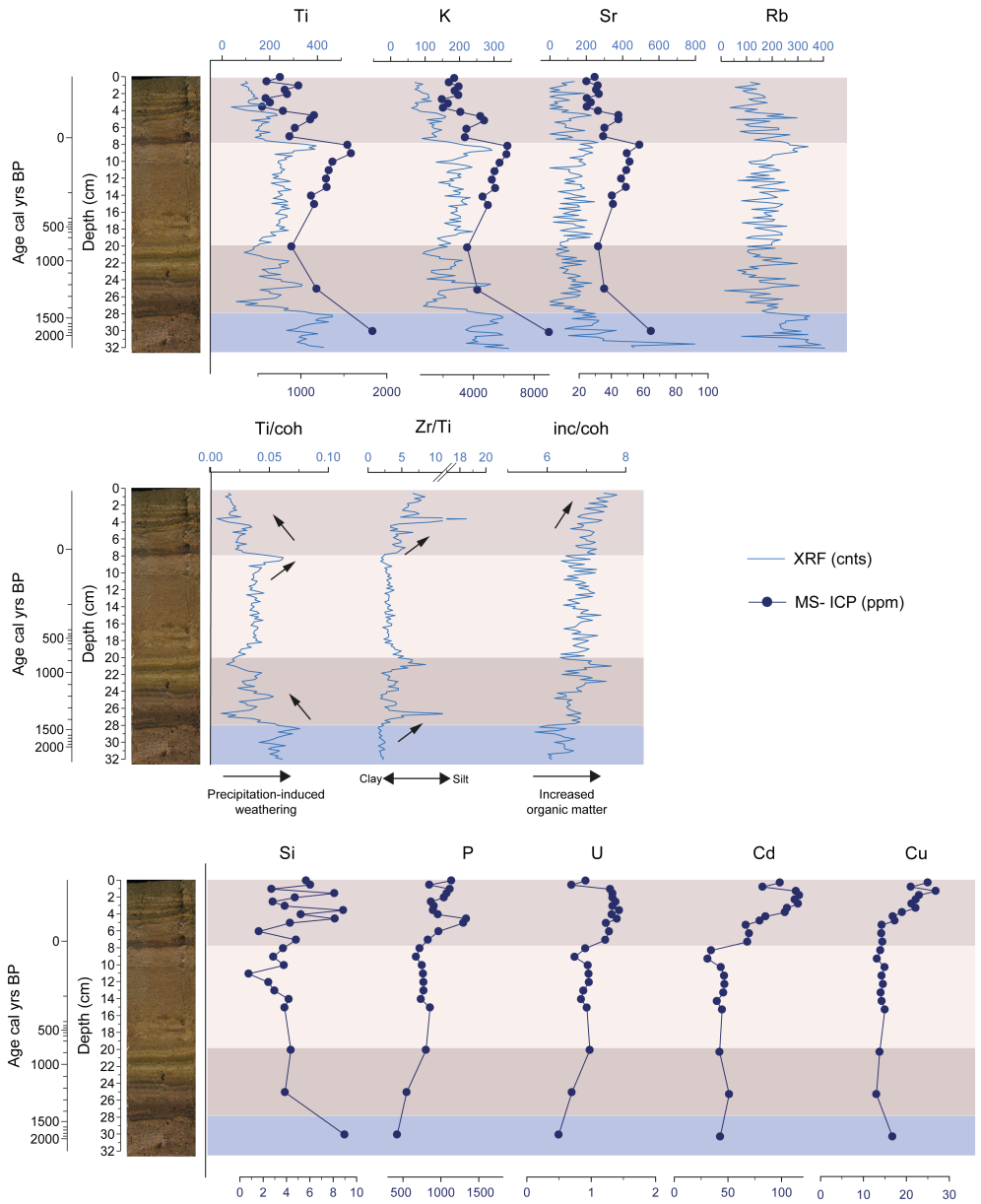

FIGURE 4
XRF and MS-ICP data of trace elements of the Laguna El Calvario.

algae *Pediastrum* and the *Zygnema* spores, values also show a significant increase whereas *Spyrogyra* spores are absent in this zone. PAR values are the highest for the whole sequence reaching up to 126 grains cm^{-2} yr^{-1}.

The diatom record of the Laguna El Calvario includes 15 taxa that have relative abundances over 5% (Figure 5B). Between 32 and 19 cm (2400–700 cal yrs BP), diatom assemblages are characterized by a high frequency of *Cymbella* spp. (20–42%), *Halamphora veneta* (15–25%) and *Gomphonema* spp. (20–50%). Associated taxa include *Planothidium aff. biporomum* (0–5%), *Pinnularia aff. brebissonii* (1–6%), *Craticula pampeana* (1–11.6% at 25–27 cm), *Craticula halophila* (0–7%), *Caloneis silicuta* (0–3%) and *Nitzchia* spp. (0–4%). Small fragilariods, including *Pseudostaurosira pseudoconstruens*, display a short-lived peak at the top of the period (ca. 1000 cal yrs BP). Diatoms abundance fluctuates between 60 and 130 × 10^7 valves per gram of dry sediment (Figure 5B). Between 19 and 5 cm (700 cal yrs BP to 1970 AD), *Gomphonema* spp. (up to 45%) and the small fragilarioids (with more than 45% at the top of the period) dominate while *Cymbella* spp. and *Halamphora veneta* values decline. Other secondary taxa such as *Fragilaria capucina* var., *Amphora copulata*, *Ulnaria ulna*, and *Encyonema silesiacum* showed minor increments. The diatom record presents a major diatom assemblage change in the last 5 cm (1970 AD to present) when most of the taxa values decline at expenses of the small fragilarioids (82–92%; Figure 5B). *Ulnaria ulna* exhibited a minor increase in the most surficial sample (5.6%).

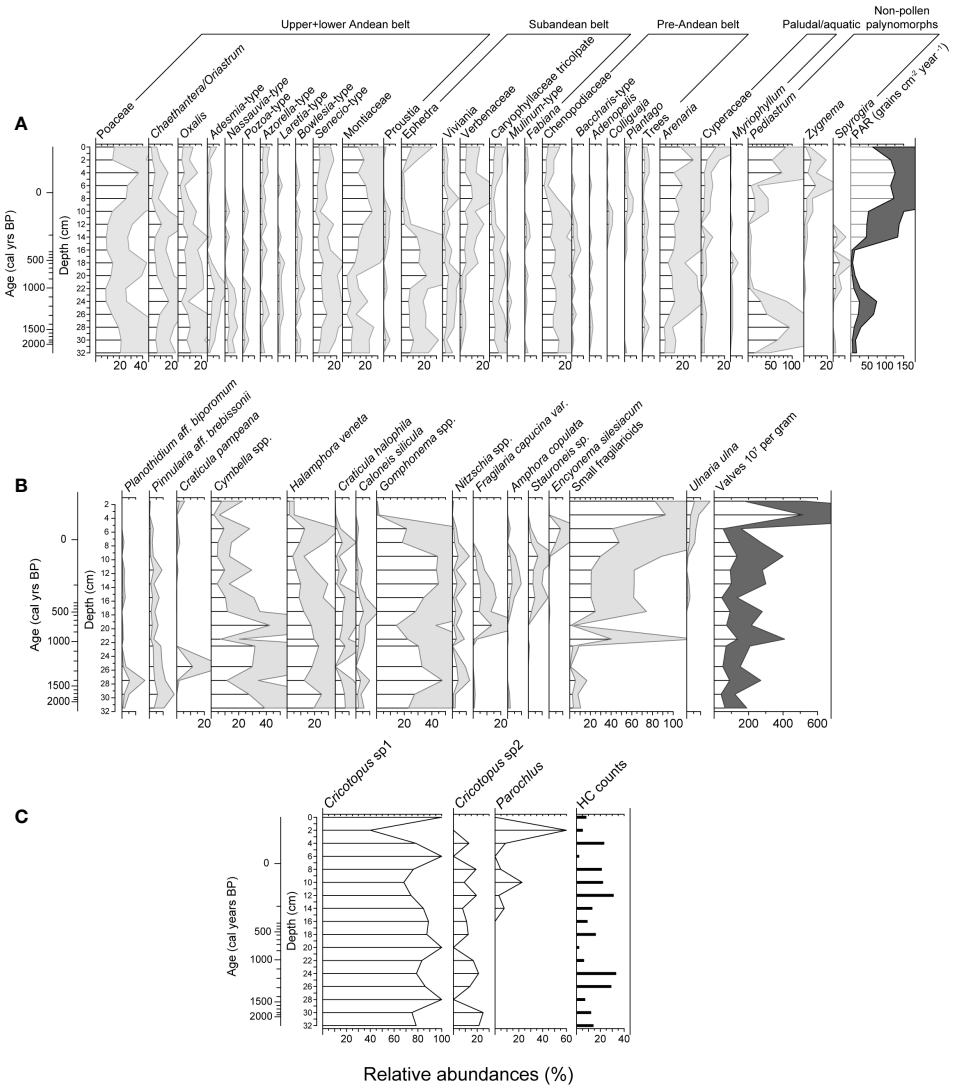

FIGURE 5
(A) Pollen record; **(B)** Diatom record; **(C)** Chironomid record of the Laguna El Calvario. The grey shadows in the pollen and diatom records correspond to exaggeration at 3x.

The chironomid record is characterized by the presence of 3 morphotypes (Figure 5C). The dominant morphotype is *Cricotopus* sp1 with ca. 80% of the total relative abundance associated with *Cricotopus* sp 2 (ca.15%) and *Parochlus* < 5%. From 32 to 14 cm (2400–120 cal yrs BP), the chironomid assemblages are dominated by the morphotypes *Cricotopus* sp1 and *Cricotopus* sp2. The Head Capsules (HC) counts are highly variable ranging between 2 and 33 (Figure 5C). Between 14 and 0 cm (from 120 cal yrs BP to 2014 AD), the chironomid record shows a clear alternation of *Cricotopus* and *Parochlus* abundance whereas the HC counts ranged from 31 and 2. *Cricotopus* sp1 dominates the whole record except for a peak of *Parochlus* at 2 cm. *Cricotopus* sp 2 co-dominates the records but disappears in the topmost 2 cm (Figure 5C). Given the low counts of HC, we interpreted with caution the chironomid record which was supported with the other proxies.

5 Discussion

5.1 Past environmental changes in Laguna El Calvario

The multiproxy analysis of Laguna El Calvario allows us to have a broad perspective of the past environmental changes during the last 2400 years in the western semiarid Andes (29°S). Following the lithological and biological changes in the sedimentary record (Figures 3–5) four main phases can be distinguished.

5.1.1 Phase 1: from 2400 to 1400 cal yr BP

Between 2400 and 1400 cal yrs BP the sedimentary record of Laguna El Calvario is characterized by the presence of sands with gravel-sized clasts (Figure 2) with high inorganic density and high values of Ti/coh ratio (particularly between 2400–2000 cal yrs BP) as

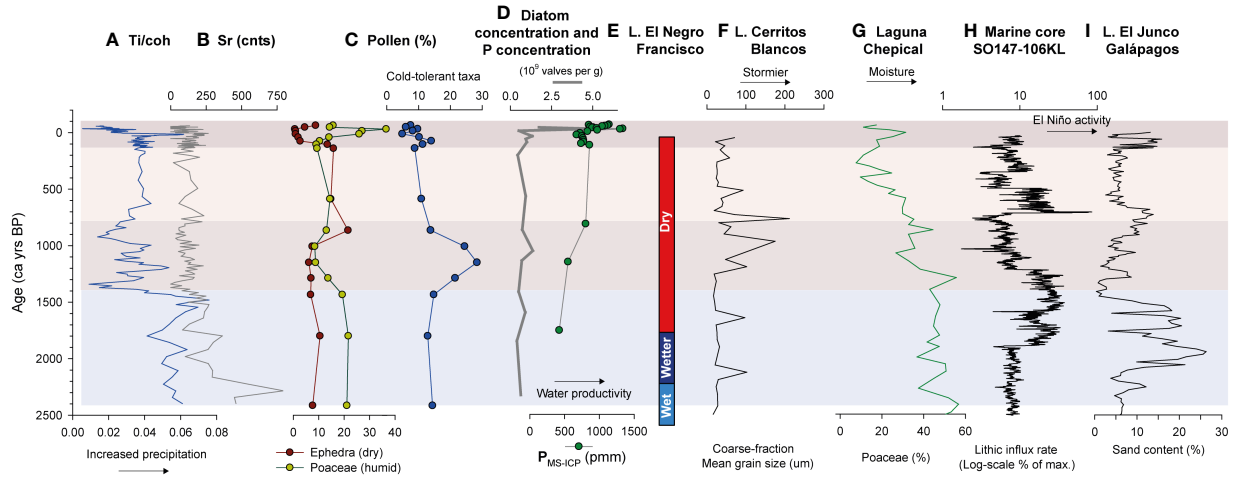

FIGURE 6
(A) Titanium/Molybdenum coherent ratio (XRF); **(B)** Sr (XRF); **(C)** Pollen; **(D)** Diatom and Phosphorus concentrations of the Laguna El Calvario; **(E)** Hydrological changes in the Andean lake Laguna El Negro Francisco (27°S; 4125 m a.s.l., Grosjean et al., 1997); **(F)** Storm activity in the Andean lake Laguna Cerritos Blancos (30°S, 3850 m a.s.l., Tiner et al., 2018); **(G)** Moisture changes in the Andean lake Laguna Chepical (32°S, 3050 m a.s.l., Martel-Cea et al., 2016); **(H)** El Niño activity inferred by Lithic influx in a sediment core located in the Peruvian offshore (Rein et al., 2005) and **(I)** Sand content in the Laguna El Junco, Galápagos archipelago, Ecuador (Conroy et al., 2008). Shadows bars correspond to the phases discussed in text.

well other elements (Figures 4, 6A, B). These sedimentological and geochemical features suggest a relatively high-energy deposition together with intense allochthonous sediment input that might be associated with high precipitation by this time (Haberzettl et al., 2005; Haberzettl et al., 2007; Schittek et al., 2016). The latter may also indicate glacial activity or increased runoff of detrital material after glacial retreatment in the basin. A similar situation has been observed in the glacial sediments from an Andean lake in Perú, where a high concentration of Sr was associated with erosion of granodiorite bedrock triggered by active glaciers (Stansell et al., 2013). More humid and colder than today conditions are reflected by the pollen record until 1400 cal yrs BP, supporting the latter. High Poaceae frequency and cold-tolerant taxa (*Chaetanthera/Oriastrum*, *Nassauvia*-type, *Adesmia*-type, *Azorella*-type, *Laretia*-type, *Senecio*-type, and Oxalis) percentages along with low pollen accumulation rates (PAR) before 1500 cal yrs BP (Figure 5A) reflect the upper Andean belt currently located 250 m above the Laguna El Calvario. However, the vegetation cover of the lower Andean belt that currently surrounds the lake catchment (4000 m a.s.l.; Figure 1) is low due to very low growth rates promoted by cold temperatures, even during the warmest months (Rudloff et al., 2021).

The diatom richness is characterized by the presence of the epiphytic diatoms *Planothidium* aff. *biporomum*, *Cymbella* spp. and *Gomphonema* spp. along with the benthic *Halamphora veneta* and *Craticula* spp. between 2400 to 1400 cal yrs BP. These assemblages reveal a shallow, vegetated, and saline-prone (particularly by the presence of *Gomphonema* spp. and *Halamphora veneta)* lacustrine environment (Figure 5B) (e.g., Jenny et al., 2002a; Jenny et al., 2002b; Hassan et al., 2013) but also the occurrence of oxygenated and shallow freshwater evidenced by the high frequency of the planktonic green algae *Pediastrum* sp. (Figure 5A) (Innes and Zong, 2021). The presence of the littoral cold-adapted *Cricotopus* as the dominant taxa in this part of the chironomid record (Figure 5C) also supports the cold and shallow conditions (Matthews-Bird et al., 2016; Motta and Massaferro, 2019; Martel-Cea et al., 2021). Additionally, the lowest values of Phosphorus and diatom concentrations may evidence low primary productivity in the water column (Figures 5B and 6D). Wet years before 1400 cal yrs BP may have increased the water input to the lake via snowmelt and/or upslope fluvio-glacial flow triggering the temporary rise of the lake level and promoting the increment of habitat opportunities for the aquatic biota (e.g., Innes and Zong, 2021).

5.1.2 Phase 2: from 1400 and 800 cal yr BP

After 1400 cal yrs BP, a shift from sand to laminated clayey silts characterized the sedimentary sequence until 800 cal yrs BP reflecting the onset of typical lacustrine-type sedimentation. The rise and fluctuation of the Zr/Ti ratio peaking around 1400–1300 and 1000–850 cal yrs BP (Figure 4) indicate an increased input of the coarser silt fraction to the lake (Oldfield et al., 2003). This might be associated with an increase in torrential rainfall, an upward displacement of the zero isotherm, or rapid melting of the snowpack as stated for the previous period. This is supported by the drop and variations of Ti/coh ratio values (Figure 6A) that imply a decrease of precipitation under a centennial-scale variability with moderate magnitude wet spells around 1200 and 1100 cal yrs BP. The pollen record shows the increment of cold-tolerant taxa (*Chaethantera/Oriastrum, Adesmia*-type, *Azorella*-type), *Arenaria* (Figure 5A), and a slight decline of Poaceae (Figure 6C) between 1400 and 800 cal yrs BP, suggesting the occurrence of cold conditions. The mild increment of PAR values (Figure 5A) can be related to an increase in temperature during the growing season (i.e., an amelioration of climatic conditions allowing the expansion of the plant cover; Squeo et al., 2006; Rudloff et al., 2021). *Arenaria* together with the persistence of *Cricotopus* spp. pointed out a decline in the lake level and/or expansion of the riparian/coastal zone (Riedemann et al., 2008; Markgraf et al., 2009; Teillier et al., 2011; Martel-Cea et al., 2016). This could be associated with a seasonal retraction of the lake that should have been constant over time in order to be recorded at sub-centennial time scales. The

aquatic taxa also point out the decline of the lake level given the sustained drop of *Pediastrum* sp. (Figure 5A). In this context, Shala et al. (2014) recorded increased Zr/Ti ratio when silt deposits in the littoral zone were eroded after the decline of the water column in a Finnish glacial lake. Therefore, the Zr/Ti increase occurred around 1350 and ca. 900 cal yrs BP in the Laguna El Calvario record could be related to an increase of detrital material by erosion and/or transport. To sum up, increased or sustained precipitation associated with cold conditions under a more pronounced seasonality occurred between 1400 and 800 cal yrs BP, compared to the previous phase.

5.1.3 Phase 3: from 800 cal yrs BP to 1850 AD

A shift from laminated to homogenous clayey silt sediment, a decline of silt influxes (low Zr/Ti ratio, Figure 4), a mild increase and stabilization of Ti/coh (Figure 6A) and other detrital input indicators (Ti, K, Sr, Ca) trends may indicate stable climatic conditions regarding the previous phase. On the other hand, the pollen record shows a minor increase of Montiaceae and *Arenaria* along with the decline of cold-tolerant taxa (*Chaethantera/ Osriastrum, Nassauvia*-type, and *Adesmia*-type) from the Andean belt associated with an expansion of shrubs from Sub-Andean (*Ephedra*, Verbenaceae) and the Pre-Andean belt pollen types (*Baccharis*) to a lesser extent (Figure 5A). This may imply an upward displacement of vegetation belts even PAR values decrease would still indicate very sparse vegetation. The increase of spores of *Spirogyra*, the absence of *Pediastrum* sp. (Figure 5A) along with the increase of the small fragilarioids between 800 and 250 cal yrs BP (Figure 5B) reveals the persistence of a shallow lake environment under dry conditions. Particularly, *Spirogyra* is common in standing water that experiences seasonal desiccation, regressive stage, and/or very shallow freshwater (Hoshaw and McCourt, 1988; Medeanic, 2006; van Geel et al., 2020). To sum up, the multiproxy record of Laguna El Calvario reflects a phase of increased aridity with an upward expansion of vegetation belts, low lake levels, and stable low precipitation between 800 cal yrs BP and 1850 AD.

5.1.4 Phase 4: from 1850 to 2014 AD

From 1850 AD to 1940 AD, the Ti/coh ratio and the allochthonous elements (Ti, K, Sr, Rb) present important peaks and then show a two-step decline during the last 50 years (Figures 4, 6A, B). In the first half of the 20th century, the PAR reached maximum values with pollen assemblages dominated by Poaceae, Montiaceae, Verbenaceae, and *Arenaria* (Figures 4A, 5C) which reflect the establishment of wetter conditions in the Laguna El Calvario basin regarding the previous phase. However, a vegetation turnover occurred in the early 2000s when lowland taxa such as Chenopodiaceae and *Ephedra* increased relative to Poaceae, Montiaceae, and *Arenaria*. This vegetation shift implies a transition from wetter than present to the current semiarid conditions that may be associated with a decrease in precipitation and a rise in temperature as recorded by instrumental records in the semiarid Andes of central Chile (Morales et al., 2020). The same trend has previously been recorded at a regional scale resulting in the glacier equilibrium line altitude, an upward shift of the zero-isotherm altitude (Carrasco et al., 2005; Barria et al., 2019), and reduction of the glacier-covered area (~35%) (Hess et al., 2020) that ultimately have directly affected the primary productivity and phenology of the Andean communities (Rudloff et al., 2021). The increment of the Zr/Ti ratio since 1940 AD (Figure 4) can be linked to the decline of the water level causing an increment of coarser silts in the sedimentary sequence accumulated in the catchment during the previous wetter decades. During the 20th century, the aquatic assemblages display the increment of *Pediastrum* sp. along with Cyperaceae and *Zygnema* (whose habitat preferences are associated with marsh environments, Figure 5A; Innes and Zong, 2021). On the other hand, the diatom assemblages display a complete dominance of the tychoplanktonic small fragilarioids and *Ulnaria ulna* (Figure 5B) whereas the chironomid record shows the establishment and increment of *Parochlus* sp., a cold-stenothermal (and an oxy-conformer) littoral taxon (Figure 5C). All the proxies together suggest a shift from a saline-prone to a cold freshwater lake probably associated with an increase of the rock glacier/snow melting along with an oxygenated (during springs) and oligo-mesotrophic water column possibly with the occurrence of ice cover during wintertime (Lotter and Bigler, 2000; Alvial et al., 2008; Hassan et al., 2013; Martel-Cea et al., 2016; Martel-Cea et al., 2021).

Recent human activity is also evident in the pollen record around Laguna El Calvario. A major increase of the palatable *Plantago* genera occurred around 1900–1920 AD (Figure 5A) synchronous to the intense transhumant livestock farming (mainly goats) that began during the first part of the 20th century (Castillo, 2003). On the other hand, even with the persistence of *Ephedra* and Chenopodiaceae throughout the record, both taxa exhibit minima values around 1900–1980 AD. *Ephedra* and Chenopodiaceae have been commonly and/or extensively used as fodder plants and/or fuel resources in the region (e.g. Meneses, 2017; Muñoz and Villaseñor, 2018) which may explain their low percentages in the pollen record during the 20th century.

High values of Ti/coh ratio, P/Ti and Si/Ti ratios (ICP-MS data), organic matter (Figures 2, 4), and diatom concentrations (Figure 6D) in the second half of the 20th century pinpoint an important increment of primary productivity. High rates of U accumulation (Figure 4) have been normally related to reducing conditions in marine and lacustrine environments which would be related to the reduction of the soluble phase of U(VI) to U(IV) in the vicinity of Fe(III) and SO_4 reduction (Klinkhammer and Palmer, 1991; Francois et al., 1993; Zheng et al., 2002; Tribovillard et al., 2006). This could explain the high concentration of U/Ti and Cd/Ti ratios, both increasing under reducing environmental conditions and in the presence of sulfides. These would have happened during periods characterized by high organic sedimentation rates which agrees with P/Ti ratio values and diatom concentration increase, reflecting the organic production in the column water or in the benthic zone. Notwithstanding, in some cases, the particulate U sedimentation overcomes the accumulation by diagenetic reactions (Chappaz et al., 2010). Instead, the Cu forms organic complexes with dissolved organic matter in superficial waters and is rapidly removed from natural waters (Rader et al., 2019). In sediments, it binds with clays, oxides, sulfides, and organic

matter (Bryan et al., 2002; Tribovillard et al., 2006) increasing the concentrations of lake bottoms when anoxic conditions prevail (Sundelin and Eriksson, 2001). In this context, the increase of Cu (shown as Cu/Ti ratio; Figure 2 Supplementary Material) would be caused by increased organic compounds in the water column derived from primary productivity within the lake and the basin. However, this coupled Cu-primary productivity increase was not observed earlier in the record. An alternative explanation could be that the metal increases could be caused by anthropogenic impact, due to in the last century mining activities, 50 km close to the lake, that has had an enormous influence on air pollution, as has been recorded both on the coast and in the Andes (von Gunten et al., 2009a; Gayo et al., 2022).

5.2 Comparing the Laguna El Calvario record at the regional scale

In order to compare the long-term environmental changes of the Laguna El Calvario (LCA) record with other paleorecords of western South America, (1) the Ti/coh ratio was selected as a proxy of runoff-induced basin erosion (Figure 6A); (2) the high Andean grassland taxa Poaceae and lowland xerophytic *Ephedra* as a moisture availability proxy while *Chaetanthera/Oriastrum*, *Adesmia* type, *Azorella* type, *Nassauvia* type as a proxy of cold conditions (Figure 6B) and; (3) the P/Ti ratio (ICP-MS) and diatom concentration as a lake productivity proxies (Figure 6C).

The relative high persistence and dominance of humid taxa throughout the pollen record of the Laguna El Calvario are consistent with the establishment of a wet Late Holocene inferred by several paleorecords in central Chile (30–35°S). Increased winter precipitation has been recorded from 4000 cal yrs BP on in the subtropical Andes (Veit, 1996; Grosjean et al., 1997; Espizua, 2005; Martel-Cea et al., 2016; Tiner et al., 2018; Frugone-Álvarez et al., 2020; Mayta and Maldonado, 2022), the lowlands (Jenny et al., 2002b; Jenny et al., 2003; Villa-Martínez et al., 2003 and Frugone-Álvarez et al., 2017) and the coastal areas (Maldonado and Villagrán, 2002 and Maldonado and Villagrán, 2006). Intense glacial activity in El Encierro valley (29°S; Figure 1A) located northwards of Laguna El Calvario was recorded before 2600 cal yrs BP (Grosjean et al., 1998; Zech et al., 2006). So after this period of glacial advance (3000–2600 yrs cal BP; Grosjean et al., 1998), the Laguna El Calvario basin could have been formed when ice retreated around 2600 cal yrs BP. High lake levels in the Laguna El Negro Francisco in the Andes at 27°S (4125 m a.s.l., Figure 6D) (Grosjean et al., 1997) and a smooth trend to wet conditions in small lakes at 30°S (3900–3800 m a.s.l.) (Mayta and Maldonado, 2022) were recorded after 2700 cal yr BP. This chronology is almost consistent with the high erosion around the lake basin (Figures 6A, B) and the downward distribution of the vegetation belts in Laguna El Calvario before 1500 cal yrs BP (Figures 4, 6C). On the other hand, grain size and geochemical analysis from two lakes located further south (Laguna El Cepo and Laguna Cerritos Blancos, 30°S, 2900–3800 m a.s.l.; Figure 1A) suggest an increment of storm frequency since 2200 cal yrs BP (Figure 6F) (Tiner et al., 2018) whereas the pollen assemblages of Laguna Quebrada Parada and Laguna Corralito (Figure 1A) pinpoint the establishment of wetter conditions from 1900 cal yrs BP (Mayta and Maldonado, 2022). Synchronous wet conditions inferred Laguna El Calvario record around 2400–1600 cal yrs BP were recorded in Laguna Chepical (32°S; Figures 1B, 6G) that shows wetter than present conditions between 2700–1300 cal yrs BP (Martel-Cea et al., 2016). Coastal and lowland records reflect wetter conditions after 3000 cal yrs BP peaking after 1800 cal yrs BP that were associated with an equatorward position/migration of the northern border of the SWW (Jenny et al., 2002a; Maldonado and Villagrán, 2002; Jenny et al., 2003).

Between 1500 and 800 cal yrs BP, the Laguna El Calvario record reflects a high variability of precipitation at the centennial scale along with the persistence of cold conditions as recorded by the dominance of high-altitude pollen types. The other paleorecords from the Elqui valley (30°S; Figure 1A) also show wetter conditions coupled with an increase in storm frequency (Tiner et al., 2018; Mayta and Maldonado, 2022). However, the Laguna Chepical record (33°S) reflects a decrease of moisture by this time but an extended ice cover season (Figure 5G) (Martel-Cea et al., 2016). In the lowlands, the Laguna Aculeo (33°S; Figure 1A) record pinpoints wet conditions between 2500–700 cal yrs BP (Villa-Martínez et al., 2003) while Palo Colorado (32°S; Figure 1A), a coastal record, displays a retraction of wet indicators around 700 cal yrs BP (Maldonado and Villagrán, 2006).

After 800–750 cal yrs BP, a marine core record located at 41°S inferred a less humid interval as a result of the southward displacement of SWW (Lamy et al., 2001) in concordance with an increase of pollen types indicating drier conditions in Laguna El Calvario, Laguna Quebrada Parada and Laguna Corralito (Mayta and Maldonado, 2022). Superimposed on these long-term conditions, a high frequency of ENOS-modulated storms was recorded by different proxies in Laguna Aculeo (33°S) and Laguna del Maule (36°S; Figure 1A) (Jenny et al., 2002a; Frugone-Álvarez et al., 2020, respectively). So, dry general climatic conditions under a high variability associated with the ENSO may have prevailed north of 32°S but more marked southwards of 33°S.

After 1800 AD, the higher temporal resolution of the Laguna El Calvario record, increasing from 0.02 to 0.13 cm yr^{-1}, provides quite detailed data for the last two centuries (Figure 2 Supplementary Material). Drier than present conditions were replaced by colder ones as reflected by the increase in upper Andean belt elements (cold-tolerant taxa) around 1850 AD. This is synchronous to the last part of the Little Ice Age, recorded in central Chile lowlands as lower spring-summer temperatures (von Gunten et al., 2009b), glacial expansion in the high Andes at 35°S (Espizua and Pitte, 2009) and increased precipitation in central Chile (33–34.5°S; LeQuesne et al., 2006). Between 1900 and 1950 AD, wet pollen indicators (Poaceae) abundance increased at the expense of cold tolerant taxa pollen. Besides, a synchronous higher variability of runoff indicators related to an upward shift of the zero-isotherm altitude might suggest an increase in liquid precipitation. This increasing trend of precipitation was also recorded by the low-frequency signal of three ring chronologies of central Chile (33°–34.5°; LeQuesne et al., 2006).

During the last part of the 20th century, similar to modern dry conditions established in Laguna El Calvario synchronously to the

mediterranean Andes (Martel-Cea et al., 2016) and the Altiplano (Morales et al., 2012). The recent decline of Poaceae and the increase of lowland shrubs (*Ephedra* and Chenopodiaceae) may represent an ongoing upward displacement of plant communities in the subtropical Andes. This process can be directly linked to the ongoing climate change characterized by the establishment of extreme drought conditions (also called Mega Drought; Garreaud et al., 2019) that broadly affects the Andean lake basins in central Chile (Fuentealba et al., 2021). Regarding regional warming, warmer autumns and springs (Burger et al., 2018) may have influenced the nutrient enrichment (high productivity, OM, and P) in Laguna El Calvario (Figure 6D; Figure 2 Supplementary Material) but may have led in a drastic decline of primary productivity in the plant communities at the same time (Rudloff et al., 2021).

Climate variability in the subtropical Andes during the late Holocene, mainly after ~2000 cal yrs BP has been attributed to El Niño Southern Oscillation, whose positive phase (El Niño) originates rainy winters in central Chile (Jenny et al., 2002a; Maldonado and Villagrán, 2006; Martel-Cea et al., 2016; Frugone-Álvarez et al., 2020). Wetter than present conditions around 2400 and 1500 cal yrs BP as well as colder conditions until 800 cal yrs BP in Laguna El Calvario is near concomitant with the increased El Niño activity inferred by several tropical records from the Eastern Pacific with a range of ca. 2000 to ca. 1000 cal yrs BP (Figures 6G, I) (Moy et al., 2002: 2000–1000 cal yrs BP; Rein et al., 2005: 2000–1300 cal yrs BP; Conroy et al., 2008: 2000–1500 cal yrs BP). Therefore, ENSO may have played a key role in the hydrological dynamics in the Laguna El Calvario at least between 2000 and 1500 cal yrs BP. Most ENSO paleorecords show a more weakened activity or La Niña-like phase in the past 800 years that may explain the stable dry conditions displayed by the Laguna El Calvario record (Moy et al., 2002; Rein et al., 2005; Conroy et al., 2008). Some discrepancies among records of central Chile and the subtropical Andes during the last millennium (i.e., Laguna Aculeo, Laguna del Maule, and neoglacial advances) could be attributed to other large atmospheric anomalies such as Southern Annular Mode (SAM) that also could have played a key role in the past at the interannual scale (Vuille and Milana, 2007; Dätwyler et al., 2020). However, further studies are needed to elucidate the implications of the coupling SAM and ENSO modes of variability in the past by evaluating the sensibility of paleorecords of the semiarid Andes of central Chile.

6 Conclusions

The Laguna El Calvario record reflects significant climate-driven changes at millennial to sub-centennial timescales during the past 2400 years in the semiarid Andes of central Chile based on sedimentological, geochemical, pollen, diatoms and chironomids data. The sediment deposition onset in Laguna El Calvario might have occurred after ice retreatment around 2600 cal yrs BP. Geochemical analyses provided a good approximation of the allochthonous clastic input where the Ti/coh ratio allowed us to estimate the long-term changes in the precipitation regime along with the pollen record. Maximum values of Ti/coh ratio evidenced an intense runoff period before 1400 cal yrs BP. Increased precipitation and colder than present conditions may have triggered a 200 m downward shift of the Andean vegetation belts whereas the aquatic biota records (algae, diatoms, and chironomids) suggested cold and shallow waters in El Calvario. Between 1500 and 800 cal yrs BP, the Laguna El Calvario record reflects wetter and colder conditions under a high centennial-to-multidecadal variability (wetter pulses) of precipitation. After 800 yrs BP, an increase of lowland pollen types in Laguna El Calvario suggests the establishment of drier conditions under a high variability associated with ENSO until 1850 AD when the dominance of upper Andean belt elements (cold tolerant taxa) indicates colder conditions synchronous to the last part of the Little Ice Age. Between 1900 and 1950 AD, an increase of wet pollen indicators at expenses of cold-tolerant taxa pollen synchronous to higher variability of runoff indicators might be related to an upward shift of the zero-isotherm altitude, and therefore a major proportion of liquid precipitation. The modern establishment of the drought regime and the increment of temperature have been shown since 1950 AD and accentuated in the last decade (Mega Drought). In addition, higher lake productivity, the presence of exotic plants, and the heavy metal enrichment of the sediments of Laguna El Calvario may be associated with transhumance practices and the establishment of the industrial mining companies in the area (Anthropocene) which have played a key role in the mid-to-long-term resilience of mountain communities.

The sedimentary record of Laguna El Calvario is not just the northernmost Andean record in central Chile but is unique in that it provides such a high temporal resolution for the last two centuries. The agreement between the Laguna El Calvario climatic trends during this period and the dendrochronological and instrumental data is surprising and confirms the robustness of this record for the whole 2400 cal yrs BP. Indeed, the regional comparison with other paleorecords allows us to confirm that even though there is a quite robust pattern of the dynamics of the northern edge of the SWW at the millennial-to-centennial scale, there are temporal (at shorter times scales)/latitudinal asynchronies that need to be further analyzed.

Data availability statement

The raw data supporting the conclusions of this article will be made available by the authors, without undue reservation.

Author contributions

All authors have approved the final version of the manuscript and the individual contributions of each co-author to the article are: AM-C analyzed the pollen, diatom, chironomid, and sedimentological data and age-depth model, wrote and edited the manuscript with contributions from all coauthors. AM designed the study, retrieved the cores, obtained the funding and participated in writing and editing the manuscript. MdP retrieved the cores, obtained the funding and participated in writing and editing the manuscript. PM carried out the ^{210}Pb chronology, the analysis of ICP-MS data and participated in writing the manuscript. NM

carried out the diatom analysis and participated in writing the manuscript. JM carried out the chironomid analysis and participated in writing the manuscript. KS carried out the XRF analysis and participated in writing the manuscript.

Funding

The author(s) declare financial support was received for the research, authorship, and/or publication of this article. The funding for this work was provided by the ANID-FONDECYT #1180413, ANID-Millennium Science Initiative Program-NCN19_153, and ANID-R20F0008.

Acknowledgments

We thank Andres Zamora for his assistance during the coring collection campaign, Leonardo D. Rios for assistance with Figure 1, Marigen Heise and Claudia Alcaíno for their assistance with laboratory analysis, Alexander Rhein for the sedimentological description, and the Hospital Público San Juan de Dios de La Serena for the digital X-ray images of the core.

Conflict of interest

The authors declare that the research was conducted in the absence of any commercial or financial relationships that could be construed as a potential conflict of interest.

Publisher's note

All claims expressed in this article are solely those of the authors and do not necessarily represent those of their affiliated organizations, or those of the publisher, the editors and the reviewers. Any product that may be evaluated in this article, or claim that may be made by its manufacturer, is not guaranteed or endorsed by the publisher.

Supplementary material

The Supplementary Material for this article can be found online at: https://www.frontiersin.org/articles/10.3389/fevo.2023.1227020/full#supplementary-material

References

Abermann, J., Kinnard, C., and MacDonell, S. (2014). Albedo variations and the impact of clouds on glaciers in the Chilean semi-arid Andes. *J. Glaciology* 60 (219), 183–191. doi: 10.3189/2014JoG13J094

Aceituno, P. (1988). On the functioning of the southern oscillation in the south american sector. Part 1: surface climate. *Monthly Weather Rev.* 116, 505–524. doi: 10.1175/1520-0493(1988)116<0505:OTFOTS>2.0.CO;2

Alvial, I., Cruces, F., Araneda, A., M., G., and R., U. (2008). Estructura comunitaria de diatomeas contenidas en el estrato superficial de ocho lagos andinos de Chile Central. *Rev. Chil. Hist. Natural* 81, 83–94. doi: 10.4067/S0716-078X2008000100007

Arroyo, M. T. K., Squeo, F. A., Armesto, J. J., and Villagrán, C. (1988). Effects of aridity on plant diversity in the northern Chilean Andes: results of a natural experiment. *Ann. Missouri Botanical Garden* 75, 55–78. doi: 10.2307/2399466

Aquino-López, M. A., Blaauw, M., and Christen, J. A. (2018). Bayesian analysis of ^{210}Pb dating. *J. Agric. Biol. Environ. Stat.* 23, 317–333. doi: 10.1007/s13253-018-0328-7

Barria, I., Carrasco, J., Casassa, G., and Barria, P. (2019). Simulation of long-term changes of the equilibrium line altitude in the central Chilean andes mountains derived from atmospheric variables during the 1958–2018 period. *Front. Environ. Sci.* 7 (161). doi: 10.3389/fenvs.2019.00161

Battarbee, R. W. (1986). "Diatoms analysis," in *Handbook of Holocene palaeoecology and palaeohydrology* (New York: John Wiley & Sons).

Blaauw, M., Christen, J. A., and Aquino-López, M. A. (2020). "rplum: bayesian age-depth modelling of '^{210}Pb'-dated cores," in *R package version 0.1.4*. Available at: https://CRAN.R-project.org/package=rplum.

Bryan, S. E., Tipping, E., and Hamilton-Taylor, J. (2002). Comparison of measured and modelled copper binding by natural organic matter in freshwaters. *Comp. Biochem. Physiol. Part C: Toxicol. Pharmacol.* 133 (1), 37–49. doi: 10.1016/S1532-0456(02)00083-2

Burger, F., Brock, B., and Montecinos, A. (2018). Seasonal and elevational contrasts in temperature trends in Central Chile between 1979 and 2015. *Global Planetary Change* 162, 136–147. doi: 10.1016/j.gloplacha.2018.01.005

Carrasco, J. F., Casassa, G., and Quintana, J. (2005). Changes of the 0°C isotherm and the equilibrium line altitude in central Chile during the last quarter of the 20th century. *Hydrological Sci. J.* 50 (6), 933–948. doi: 10.1623/hysj.2005.50.6.933

Castillo, G. (2003). "La vuelta de los años: reseñas y perspectivas sobre las comunidades, el pastoreo y la tranhumancia en la región semiárida de Chile," in *Dinámicas de los sistemas agrarios en el Chile árido: la Región de Coquimbo. Santiago*. Eds. P. Livenais and X. Aranda (Santiago de Chile: LOM Ediciones), 65–116.

Chappaz, A., Gobeil, C., and Tessier, A. (2010). Controls on uranium distribution in lake sediments. *Geochimica Cosmochimica Acta* 74 (1), 203–214. doi: 10.1016/j.gca.2009.09.026

Conroy, J. L., Overpeck, J. T., Cole, J. E., Shanahan, T. M., and Steinitz-Kannan, M. (2008). Holocene changes in eastern tropical Pacific climate inferred from a Galápagos lake sediment record. *Quaternary Sci. Rev.* 27 (11), 1166–1180. doi: 10.1016/j.quascirev.2008.02.015

Cranston, P. S. (2019). Identification guide to genera of aquatic larval Chironomidae (Diptera) of Australia and New Zealand. *Zootaxa* 4706 (1), 071–102. doi: 10.11646/zootaxa.4706.1.3

Croudace, I. W., Rindby, A., Rothwell, R. G., and Rothwell, R. G. (2006). "ITRAX: description and evaluation of a new multi-function X-ray core scanner," in *New techniques in sediment core analysis*. Ed. R. G. Rothwell (London: Geological Society of London), 51–63.

Dätwyler, C., Grosjean, M., Steiger, N. J., and Neukom, R. (2020). Teleconnections and relationship between the El Niño–Southern Oscillation (ENSO) and the Southern Annular Mode (SAM) in reconstructions and models over the past millennium. *Clim. Past* 16 (2), 743–756. doi: 10.5194/cp-16-743-2020

Davies, S. J., Lamb, H. F., and Roberts, S. J. (2015). "Micro-XRF core scanning in palaeolimnology: recent developments," in *Micro-XRF Studies of Sediment Cores: Applications of a non-destructive tool for the environmental sciences*. Eds. I. W. Croudace and R. G. Rothwell (Dordrecht: Springer Netherlands), 189–226.

Emanuelli, P., Milla, F., Duarte, E., Torrealba, J., Garrido Ruiz, C., Colmenares, M., et al. (2016). "Diagnóstico de la desertificación en Chile y sus efectos en el desarrollo sustentable. Technical report 03," (Santiago, Chile: Corporación Nacional Forestal (CONAF)) 33 pp. Available at: https://bibliotecadigital.ciren.cl/handle/20.500.13082/32893. (Accessed November 23, 2023).

Espizua, L. E. (2005). Holocene glacier chronology of Valenzuela Valley, Mendoza Andes, Argentina. *Palaeogeogr., Palaeoclimatol., Palaeoecol.* 15 (7), 1079–1085. doi: 10.1191/0959683605hl866rr

Espizua, L. E., and Pitte, P. (2009). The Little Ice Age glacier advance in the Central Andes (35°S), Argentina. *Palaeogeography, Palaeoclimatology, Palaeoecology* 281, 345–350. doi: 10.1016/j.palaeo.2008.10.032

Faegri, K., and Iversen, J. (1989). *Textbook of pollen analysis* (Londres: John Wiley & Sons Ld).

Falvey, M., and Garreaud, R. D. (2007). Wintertime precipitation episodes in central Chile: associated meteorological conditions and orographic influences. *J. Hydrometeorology* 8, 171–193. doi: 10.1175/JHM562.1

Falvey, M., and Garreaud, R. D. (2009). Regional cooling in a warming world: Recent temperature trends in the southeast Pacific and along the west coast of subtropical South America, (1979-2006). *J. Geophysical Res.* 114 (D4), D04102. doi: 10.1029/2008jd010519

Flynn, W. (1968). The determination of low levels of polonium-210 in environmental materials. *Analytica chimica Acta* 43, 221–226. doi: 10.1016/S0003-2670(00)89210-7

Francois, R., Bacon, M. P., Altabet, M. A., and Labeyrie, L. D. (1993). Glacial/interglacial changes in sediment rain rate in the SW Indian Sector of subantarctic Waters as recorded by 230Th, 231Pa, U, and δ15N. *Paleoceanography* 8 (5), 611–629. doi: 10.1029/93PA00784

Frugone-Álvarez, M., Latorre, C., Barreiro-Lostres, F., Giralt, S., Moreno, A., Polanco-Martínez, J., et al. (2020). Volcanism and climate change as drivers in Holocene depositional dynamic of Laguna del Maule (Andes of central Chile – 36° S). *Clim. Past* 16 (4), 1097–1125. doi: 10.5194/cp-16-1097-2020

Frugone-Álvarez, M., Latorre, C., Giralt, S., Polanco-Martínez, J., Bernárdez, P., Oliva-Urcia, B., et al. (2017). A 7000-year high-resolution lake sediment record from coastal central Chile (Lago Vichuquén, 34°S): implications for past sea level and environmental variability. *J. Quaternary Sci.* 32 (6), 830–844. doi: 10.1002/jqs.2936

Fuentealba, M., Bahamóndez, C., Sarricolea, P., Meseguer-Ruiz, O., and Latorre, C. (2021). The 2010–2020 'megadrought' drives reduction in lake surface area in the Andes of central Chile (32° - 36°S). *J. Hydrology: Regional Stud.* 38, 100952. doi: 10.1016/j.ejrh.2021.100952

Garreaud, R. D. (2009). The Andes climate and weather. *Advanced Geosciences* 22, 3–11. doi: 10.5194/adgeo-22-3-2009

Garreaud, R. D., Boisier, J. P., Rondanelli, R., Montecinos, A., Sepúlveda, H. H., and Veloso-Aguila, D. (2019). The central Chile mega drought (2010–2018): A climate dynamics perspective. *Int. J. Climatology* 40 (1), 421–439. doi: 10.1002/joc.6219

Garreaud, R. D., and Rutllant, J. (1997). Precipitación estival en los Andes de Chile central: Aspectos climatológicos. *Atmósfera* 10, 191–211. Available at: https://www.revistascca.unam.mx/atm/index.php/atm/article/view/8418.

Gascoin, S., Kinnard, C., Ponce, R., Lhermitte, S., MacDonell, S., and Rabatel, A. (2011). Glacier contribution to streamflow in two headwaters of the Huasco River, Dry Andes of Chile. *Cryosphere* 5 (4), 1099–1113. doi: 10.5194/tc-5-1099-2011

Gayo, E. M., Muñoz, A. A., Maldonado, A., Lavergne, C., Francois, J. P., Rodríguez, D., et al. (2022). A cross-cutting approach for relating Anthropocene, environmental injustice and sacrifice zones. *Earth's Future* 10, e2021EF002217. doi: 10.1029/2021EF002217

Grosjean, M., Geyh, M. A., Messerli, B., Schreier, H., and Veit, H. (1998). A late-Holocene (<2600 BP) glacial advance in the south-central Andes (29°S), northern Chile. *Holocene* 8 (4), 473–479. doi: 10.1191/095968398677627864

Grosjean, M., Valero-Garcés, B. L., Geyh, M. A., Messerli, B., Schotterer, U., Schreier, H., et al. (1997). Mid- and late-Holocene limnogeology of Laguna del Negro Francisco, northern Chile, and its palaeoclimatic implications. *Holocene* 7 (2), 151–159. doi: 10.1177/095968369700700203

Guyard, H., Chapron, E., St-Onge, G., Anselmetti, F. S., Arnaud, F., Magand, O., et al. (2007). High-altitude varve records of abrupt environmental changes and mining activity over the last 4000 years in the Western French Alps (Lake Bramant, Grandes Rousses Massif). *Quat. Sci. Rev.* 26 (19), 2644–2660. doi: 10.1016/j.quascirev.2007.07.007

Haberzettl, T., Corbella, H., Fey, M., Janssen, S., Lücke, A., Mayr, C., et al. (2007). Lateglacial and Holocene wet—dry cycles in southern Patagonia: chronology, sedimentology and geochemistry of a lacustrine record from Laguna Potrok Aike, Argentina. *Holocene* 17 (3), 297–310. doi: 10.1177/0959683607076437

Haberzettl, T., Fey, M., Lücke, A., Maidana, N., Mayr, C., Ohlendorf, C., et al. (2005). Climatically induced lake level changes during the last two millennia as reflected in sediments of Laguna Potrok Aike, southern Patagonia (Santa Cruz, Argentina). *J. Paleolimnology* 33 (3), 283–302. doi: 10.1007/s10933-004-5331-z

Hassan, G. S., De Francesco, C. G., and Dieguez, S. (2013). The significance of modern diatoms as paleoenvironmental indicators along an altitudinal gradient in the Andean piedmont of central Argentina. *Palaeogeography Palaeoclimatology Palaeoecol.* 369 (0), 349–360. doi: 10.1016/j.palaeo.2012.11.002

Heiri, O., Lotter, A., and Lemcke, G. (2001). Loss on ignition as a method for estimating organic and carbonate content in sediments: reproducibility and comparability of results. *J. Paleolimnology* 25, 101–110. doi: 10.1023/A:1008119611481

Hess, K., Schmidt, S., Nüsser, M., Zang, C., and Dame, J. (2020). Glacier changes in the semi-arid huasco valley, Chile, between 1986 and 2016. *Geosciences* 10 (11), 429. doi: 10.3390/geosciences10110429

Heusser, C. J. (1971). *Pollen and spores of Chile: Modern types of the Pteridophyta, Gymnospermae, and Angiospermae* (Tucson: University of Arizona Press).

Hogg, A. G., Heaton, T. J., Hua, Q., Palmer, J. G., Turney, C. S. M., Southon, J., et al. (2020). SHCal20 southern hemisphere calibration, 0–55,000 years cal BP. *Radiocarbon* 62 (4), 759–778. doi: 10.1017/RDC.2020.59

Hoshaw, R. W., and McCourt, R. M. (1988). The Zygnemataceae (Chlorophyta): a twenty-year update of research. *Phycologia* 27 (4), 511–548. doi: 10.2216/i0031-8884-27-4-511.1

Innes, J. B., and Zong, Y. (2021). History of mid- and late holocene palaeofloods in the yangtze coastal lowlands, east China: evaluation of non-pollen palynomorph evidence, review and synthesis. *Quaternary* 4 (3), 21. doi: 10.3390/quat4030021

Jenny, B., Valero-Garcés, B. L., Urrutia, R., Kelts, K., Veit, H., Appleby, P. G., et al. (2002a). Moisture changes and fluctuations of the Westerlies in Mediterranean Central Chile during the last 2000 years: The Laguna Aculeo record (33°50'S). *Quaternary Int.* 87 (1), 3–18. doi: 10.1016/s1040-6182(01)00058-1

Jenny, B., Valero-Garcés, B. L., Villa-Martínez, R., Urrutia, R., Geyh, M., and Veit, H. (2002b). Early to mid-holocene aridity in central Chile and the southern westerlies: the laguna aculeo record (34°S). *Quaternary Res.* 58 (2), 160–170. doi: 10.1006/qres.2002.2370

Jenny, B., Wilhelm, D., and Valero-Garcés, B. L. (2003). The Southern Westerlies in Central Chile: Holocene precipitation estimates based on a water balance model for Laguna Aculeo (33°50'S). *Climate Dynamics* 20 (2), 269–280. doi: 10.1007/s00382-002-0267-3

Klinkhammer, G. P., and Palmer, M. R. (1991). Uranium in the oceans: Where it goes and why. *Geochimica Cosmochimica Acta* 55 (7), 1799–1806. doi: 10.1016/0016-7037(91)90024-Y

Lamy, F., Hebbeln, D., Röhl, U., and Wefer, G. (2001). Holocene rainfall variability in southern Chile: a marine record of latitudinal shifts of the Southern Westerlies. *Earth Planetary Sci. Lett.* 185 (3-4), 369–382. doi: 10.1016/s0012-821x(00)00381-2

Lange-Bertalot, H., Hofmann, G., Werum, M., and Cantonati, M. (2017). "Freshwater Benthic Diatoms of Central Europe. Over 800 common species used in ecological assessment. English edition with updated taxonomy and added species," Schmitten-Oberreifenberg (Germany): Koeltz Botanical Books.

LeQuesne, C., Stahle, D. W., Cleaveland, M. K., Therrell, M. D., Aravena, J. C., and Barichivich, J. (2006). Ancient austrocedrus tree-ring chronologies used to reconstruct central Chile precipitation variability from A.D. 1200 to 2000. *J. Clim.* 19, 5731-5744. doi: 10.1175/jcli3935.1

López-Angulo, J., Pescador, D. S., Sánchez, A. M., Mihoč, M. A. K., Cavieres, L. A., and Escudero, A. (2018). Determinants of high mountain plant diversity in the Chilean Andes: From regional to local spatial scales. *PloS One* 13 (7), e0200216. doi: 10.1371/journal.pone.0200216

Lotter, A. F., and Bigler, C. (2000). Do diatoms in the Swiss Alps reflect the length of ice-cover? *Aquat. Sci.* 62 (2), 125–141. doi: 10.1007/s000270050002

Luebert, F., and Pliscoff, P. (2017). *Sinopsis bioclimática y vegetacional de Chile.* (Santiago, Chile: Editorial Universitaria).

Maldonado, A., and Villagrán, C. (2002). Paleoenvironmental Changes in the Semiarid Coast of Chile (~32°S) during the Last 6200 cal Years Inferred from a Swamp-Forest Pollen Record. *Quaternary Res.* 58 (2), 130–138. doi: 10.1006/qres.2002.2353

Maldonado, A., and Villagrán, C. (2006). Climate variability over the last 9900 cal yr BP from a swamp forest pollen record along the semiarid coast of Chile. *Quaternary Res.* 66 (2), 246–258. doi: 10.1016/j.yqres.2006.04.003

Markgraf, V., and D'Antoni, H. L. (1978). *Pollen Flora of Argentina. Modern Spores and Pollen Types of Pteridophyta, Gymnospermae and Angiospermae.* (Tucson: The University of Arizona Press).

Markgraf, V., Whitlock, C., Anderson, R. S., and Garcia, A. (2009). Late Quaternary vegetation and fire history in the northernmost Nothofagus forest region: Mallin Vaca Lauquen, Neuquen Province, Argentina. *J. Quaternary Sci.* 24 (3), 248–258. doi: 10.1002/jqs.1233

Martel-Cea, A., Astorga, G. A., Hernández, M., Caputo, L., and Abarzúa, A. M. (2021). Modern chironomids (Diptera: Chironomidae) and the environmental variables that influence their distribution in the Araucanian lakes, south-central Chile. *Hydrobiologia* 848 (10), 2551–2568. doi: 10.1007/s10750-021-04575-0

Martel-Cea, A., Maldonado, A., Grosjean, M., Alvial, I., de Jong, R., Fritz, S. C., et al. (2016). Late Holocene environmental changes as recorded in the sediments of high Andean Laguna Chepical, Central Chile (32°S; 3050 m a.s.l.). *Palaeogeography Palaeoclimatology Palaeoecol.* 461, 44–54. doi: 10.1016/j.palaeo.2016.08.003

Masiokas, M., Villalba, R., Luckman, B. H., Le Quesne, C., and Aravena, J. C. (2006). Snowpack variations in the central andes of Argentina and Chile 1951 2005: large-scale atmospheric influences and implications for water resources in the region. *J. Climate* 19, 6634–6352. doi: 10.1175/JCLI3969.1

Massaferro, J., and Brooks, S. J. (2002). Response of chironomids to Late Quaternary environmental change in the Taitao Peninsula, southern Chile. *J. Quaternary Sci.* 17 (2), 101–111. doi: 10.1002/jqs.671

Massaferro, J., Ortega, C., Fuentes, R., and Araneda, A. (2013). Guia Para la Identificación de Tanytarsini Subfosiles (Diptera: Chironomidae: Chironominae) de la Patagonia. *Ameghiniana* 50 (3), 319–334. doi: 10.5710/amgh.05.03.2013.566

Matthews-Bird, F., Gosling, W. D., Coe, A. L., Bush, M., Mayle, F. E., Axford, Y., et al. (2016). Environmental controls on the distribution and diversity of lentic Chironomidae (Insecta: Diptera) across an altitudinal gradient in tropical South America. *Ecol. Evol.* 6 (1), 91–112. doi: 10.1002/ece3.1833

Mayta, C., and Maldonado, A. (2022). Climatic and ecological changes in the subtropical high Andes during the last 4,500 years. *Front. Earth Sci.* 10, 833219. doi: 10.3389/feart.2022.833219

Medeanic, S. (2006). Freshwater algal palynomorph records from Holocene deposits in the coastal plain of Rio Grande do Sul, Brazil. *Rev. Palaeobotany Palynology* 141 (1), 83–101. doi: 10.1016/j.revpalbo.2006.03.012

Meneses, R. (2017). Manual de produccion caprina [en línea]. In: *Boletin INIA - Instituto de Investigaciones Agropecuarias*. Available at: https://hdl.handle.net/20.500.14001/6672 (Accessed 18-07-2022).

Metzeltin, D., and Lange-Bertalot, H. (1998). Tropical diatoms of South America I. About 700 predominantly rarely known or new taxa representative of the neotropical flora. *Iconogr Diatomol* 5, 1–695.

Metzeltin, D., and Lange-Bertalot, H. (2007). Tropical diatoms of South America II. Special remarks on biogeographic disjunction. *Iconogr Diatomol* 18, 1–877.

Mondal, M. N., Horikawa, K., Seki, O., Nejigaki, K., Minami, H., Murayama, M., et al. (2021). Investigation of adequate calibration methods for X-ray fluorescence core scanning element count data: A case study of a marine sediment piston core from the Gulf of Alaska. *J. Mar. Sci. Eng.* 9 (5), 540. doi: 10.3390/jmse9050540

Montecinos, A., and Aceituno, P. (2003). Seasonality of the ENSO-related rainfall variability in central Chile and associated circulation anomalies. *J. Climate* 16 (2), 281–296. doi: 10.1175/1520-0442(2003)016<0281:SOTERR>2.0.CO;2

Morales, M. S., Christie, D. A., Villalba, R., Argollo, J., Pacajes, J., Silva, J. S., et al. (2012). Precipitation changes in the South American Altiplano since 1300 AD reconstructed by tree-rings. *Clim. Past* 8 (2), 653–666. doi: 10.5194/cp-8-653-2012

Morales, M. S., Cook, E. R., Barichivich, J., Christie, D. A., Villalba, R., LeQuesne, C., et al. (2020). Six hundred years of South American tree rings reveal an increase in severe hydroclimatic events since mid-20th century. *PNAS* 117 (29), 16816–16823. doi: 10.1073/pnas.2002411117

Motta, L., and Massaferro, J. (2019). Climate and site-specific factors shape chironomid taxonomic and functional diversity patterns in northern Patagonia. *Hydrobiologia* 839 (1), 131–143. doi: 10.1007/s10750-019-04001-6

Moy, C. M., Seltzer, G. O., Rodbell, D. T., and Anderson, D. M. (2002). Variability of El Nino/Southern Oscillation activity at millennial timescales during the Holocene epoch. *Nature* 420 (6912), 162–165.

Muñoz, P., Rebolledo, L., Dezileau, L., Maldonado, A., Mayr, C., Cárdenas, P., et al. (2020). Reconstructing past variations in environmental conditions and paleoproductivity over the last ~8000 years off north-central Chile (30° S). *Biogeosciences* 17 (22), 5763–5785. doi: 10.5194/bg-17-5763-2020

Muñoz, E. J., and Villaseñor, R. (2018). Uso de las plantas nativas por una comunidad de cabreros de Las Vegas de la quebrada de Tulahuén, Región de Coquimbo, Chile. *Idesia (Arica)* 36 (2), 243–258. doi: 10.4067/S0718-34292018005000201

Murillo, I., Velásquez, R., and Creixell, T. (2017). *Geología de la Áreas Guanta - Los Cuartitos y Paso de Vacas Heladas, Regiones de Atacama y Coquimbo. Escala 1: 100.000.* (Santiago de Chile: SERNAGEOMIN).

Nasi, C., Mpodozis, C., Moscoso, R., Maksaev, V., and Cornejo, P. (1985). El Batolito Elqui-Limarí (Paleozoico Superior-Triásico): características petrográficas, geoquímicas y significado tectónico. *Rev. Geológica Chile* 25-26, 77–111. doi: 10.5027/andgeoV12n2-3-a06

Ohlendorf, C., Fey, M., Massaferro, J., Haberzettl, T., Laprida, C., Lücke, A., et al. (2014). Late Holocene hydrology inferred from lacustrine sediments of Laguna Cháltel (southeastern Argentina). *Palaeogeography Palaeoclimatology Palaeoecol.* 411, 229–248. doi: 10.1016/j.palaeo.2014.06.030

Oldfield, F., Wake, R., Boyle, J., Jones, R., Nolan, S., Gibbs, Z., et al. (2003). The late-Holocene history of Gormire Lake (NE England) and its catchment: a multiproxy reconstruction of past human impact. *Holocene* 13 (5), 677–690. doi: 10.1191/0959683603hl654rp

Oyarzún, R., Lillo, J., Oyarzún, J., Higueras, P., and Maturana, H. (2006). Strong metal anomalies in stream sediments from semiarid watersheds in Northern Chile: When geological and structural analyses contribute to understanding environmental disturbances. *Int. Geology Rev.* 48 (12), 1133–1144. doi: 10.2747/0020-6814.48.12.1133

Pizarro-Tapia, R., Ibáñez-Córdova, A., García-Chevesich, P., Vallejos-Carrera, C., Sangüesa-Pool, C., and Mendoza-Mendoza, R. (2021). "The Chilean forest sector and its relationship with water resources," in *Water Resources of Chile*. Eds. B. Fernández and J. Gironás (Cham: Springer International Publishing), 301–315.

Quintana, J., and Aceituno, P. (2012). Changes in the rainfall regime along the extratropical west coast of South America (Chile): 30-43° S. *Atmosfera* 25 (1), 1–22. Available at: https://www.redalyc.org/articulo.oa?id=56523435001 (Accessed November 23, 2023).

Rader, K. J., Carbonaro, R. F., van Hullebusch, E. D., Baken, S., and Delbeke, K. (2019). The fate of copper added to surface water: field, laboratory, and modeling studies. *Environ. Toxicol. Chem.* 38 (7), 1386–1399. doi: 10.1002/etc.4440

Rein, B., Lückge, A., Reinhardt, L., Sirocko, F., Wolf, A., and Dullo, W.-C. (2005). El Niño variability off Peru during the last 20,000 years. *Paleoceanography* 20 (4), PA4003. doi: 10.1029/2004pa001099

Riedemann, P., Aldunate, G., and Teillier, S. (2008). *Flora nativa de valor ornamental: Chile zona Cordillera de Los Andes. Identificación y propagación* (Santiago, Chile: Corporación Jardín Botánico Chagual).

Rudloff, V. M., Rutllant, J. A., Martel-Cea, A., and Maldonado, A. (2021). Hydrothermal modulation of NDVI in the high-altitude semiarid Andes of Chile (30–34°S). *J. Arid Environments* 186, 104397. doi: 10.1016/j.jaridenv.2020.104397

Rumrich, U., Lange-Bertalot, H., and Rumrich, M. (2000). Diatoms of the Andes. From Venezuela to Patagonia/Tierra del Fuego. *Iconogr. Diatomol.* 9, 7–649.

Schittek, K., Kock, S. T., Lücke, A., Hense, J., Ohlendorf, C., Kulemeyer, J. J., et al. (2016). A high-altitude peatland record of environmental changes in the NW Argentine Andes (24 °S) over the last 2100 years. *Clim. Past* 12 (5), 1165–1180. doi: 10.5194/cp-12-1165-2016

SERPLAC. (1986). *La Minería en la IV región. Secretaría Regional de Planificación y Coordinación IV región*. (La Serena, Chile: Intendencia Región Coquimbo). 33 p. Available at: https://bibliotecadigital.ciren.cl/handle/20.500.13082/25817. Last access: (Accessed November 23, 2023).

Shala, S., Helmens, K. F., Jansson, K. N., Kylander, M. E., Risberg, J., and Löwemark, L. (2014). Palaeoenvironmental record of glacial lake evolution during the early Holocene at Sokli, NE Finland. *Boreas* 43 (2), 362–376. doi: 10.1111/bor.12043

Squeo, F. A., Osorio, R., and Arancio, G. (1994). *Flora de Los Andes de Coquimbo: Cordillera de Doña Ana.* (La Serena: Universidad de la Serena).

Squeo, F. A., Tracol, Y., López, D., Gutiérrez, J. R., Cordova, A. M., and Ehleringer, J. R. (2006). ENSO effects on primary productivity in Southern Atacama desert. *Advanced Geosciences* 6, 273–277. doi: 10.5194/adgeo-6-273-2006

Squeo, F. A., Veit, H., Arancio, G., Gutierrez, J. R., Arroyo, M. T. K., and Olivares, N. (1993). Spatial heterogeneity of high mountain vegetation in the andean desert zone of Chile. *Mountain Res. Dev.* 13 (2), 203–209. doi: 10.2307/3673638

Stansell, N. D., Rodbell, D. T., Abbott, M. B., and Mark, B. G. (2013). Proglacial lake sediment records of Holocene climate change in the western Cordillera of Peru. *Quaternary Sci. Rev.* 70, 1–14. doi: 10.1016/j.quascirev.2013.03.003

Stockmarr, J. (1971). Tablets with spores used in absolute pollen analysis. *Pollen spores* 13, 615–621.

Sundelin, B., and Eriksson, A.-K. (2001). *Environ. Toxicol. Chem.* 20 (4), 748–756. doi: 10.1002/etc.5620200408

Teillier, S., Marticorena, A., and Niemeyer, H. (2011). *Flora Andina de Santiago. Guía para la identificación de las especies de las cuencas del Maipo y del Mapocho.* (Santiago: Universidad de Chile).

Tiner, R. J., Negrini, R. M., Antinao, J. L., McDonald, E., and Maldonado, A. (2018). Geophysical and geochemical constraints on the age and paleoclimate implications of Holocene lacustrine cores from the Andes of central Chile. *J. Quaternary Sci.* 33 (2), 150–165. doi: 10.1002/jqs.3012

Tribovillard, N., Algeo, T. J., Lyons, T., and Riboulleau, A. (2006). Trace metals as paleoredox and paleoproductivity proxies: An update. *Chem. Geology* 232 (1), 12–32. doi: 10.1016/j.chemgeo.2006.02.012

van Geel, B., Brinkkemper, O., van Reenen, G. B. A., Van der Putten, N. N. L., Sybenga, J. E., Soonius, C., et al. (2020). Multicore study of upper holocene mire development in west-frisia, northern Netherlands: ecological and archaeological aspects. *Quaternary* 3 (2), 12. doi: 10.3390/quat3020012

Veit, H. (1996). Southern Westerlies during the Holocene deduced from geomorphological and pedological studies in the Norte Chico, Northern Chile (27-33°S). *Palaeogeography Palaeoclimatology Palaeoecol.* 123 (1-4), 107–119. doi: 10.1016/0031-0182(95)00118-2

Viale, M., and Garreaud, R. (2014). Summer precipitation events over the western slope of the subtropical Andes. *Mon. Wea. Rev.* 142, 1074–1092. doi: 10.1175/MWR-D-13-00259.1

Vicuña, S., Garreaud, R., and McPhee, J. (2011). Climate change impacts on the hydrology of a snowmelt driven basin in semiarid Chile. *Climatic Change* 105 (3), 469–488. doi: 10.1007/s10584-010-9888-4

Villagrán, C., Arroyo, M. T. K., and Marticorena, R. (1983). Efectos de la desertización en la distribución de la flora andina de Chile. *Rev. Chil. Hist. Natural* 56, 137–157.

Villa-Martínez, R., Villagrán, C., and Jenny, B. (2003). The last 7500 cal yr B.P. of westerly rainfall in Central Chile inferred from a high-resolution pollen record from Laguna Aculeo (34°S). *Quaternary Res.* 60 (3), 284–293. doi: 10.1016/j.yqres.2003.07.007

von Gunten, L., Grosjean, M., Eggenberger, U., Grob, P., Urrutia, R., and Morales, A. (2009a). Pollution and eutrophication history AD 1800–2005 as recorded in sediments from five lakes in Central Chile. *Global Planetary Change* 68 (3), 198–208. doi: 10.1016/j.gloplacha.2009.04.004

von Gunten, L., Grosjean, M., Rein, B., Urrutia, R., and Appleby, P. (2009b). A quantitative high-resolution summer temperature reconstruction based on sedimentary pigments from Laguna Aculeo, central Chile, back to AD 850. *Holocene* 19, 873–881. doi: 10.1177/0959683609336573

Vuille, M., and Milana, J. P. (2007). High-latitude forcing of regional aridification along the subtropical west coast of South America. *Geophysical Res. Lett.* 34 (23), L23703. doi: 10.1029/2007gl031899

Zech, R., Kull, C., and Veit, H. (2006). Late Quaternary glacial history in the Encierro Valley, northern Chile (29°S), deduced from 10Be surface exposure dating. *Palaeogeography Palaeoclimatol. Palaeoecol.* 234 (2), 277–286. doi: 10.1016/j.palaeo.2005.10.011

Zhang, X., Zhang, H., Chang, F., Ashraf, U., Peng, W., and Wu, H. (2020). Application of corrected methods for high-resolution XRF core scanning elements in lake sediments. *Appl. Sci.* 10 (22), 8012. doi: 10.3390/app10228012

Zheng, Y., Anderson, R. F., van Geen, A., and Fleisher, M. Q. (2002). Preservation of particulate non-lithogenic uranium in marine sediments. *Geochimica Cosmochimica Acta* 66 (17), 3085–3092. doi: 10.1016/S0016-7037(01)00632-9